Agricultural and Forest Meteorology 376 (2026) 110903

Contents lists available at ScienceDirect

Agricultural and Forest Meteorology

journal homepage: www.elsevier.com/locate/agrformet

A series-scheme surface-renewal method within a two-source energy-balance framework

Francesc Castellví [a,*], María P. González-Dugo [b]

[a] Department of Chemistry, Physics, Environment and Soil Sciences, University of Lleida, Lleida, Spain
[b] IFAPA. Institute of Agricultural and Fisheries Research and Training of Andalusia Avd. Menéndez Pidal s/n, 14071 Cordoba, Spain

ARTICLE INFO

Keywords:
Surface renewal
Two-source energy balance (TSEB)
Sensible heat flux
Series scheme
Remote sensing

ABSTRACT

A new technique, based on Surface Renewal (SR), was developed to explain the contribution of the soil and the vegetation of the sensible heat flux. It was compared to the original Two Source Energy Balance (TSEB) model based on series scheme. The methodology to partition the components of the radiation, the soil heat flux and the latent heat flux for the soil and vegetation were identical to the original model, however, the SR concepts were implemented to estimate the sensible heat flux over sparse canopies. The key point was to model the temperature of the macro-parcel of air during the quiescent period. The input requirements are the same as the original model. The TSEB model was tested half-hourly under clear sky conditions and unstable cases for two growing crops (rain-fed soybean and corn using 12 and 14 samples, respectively) with canopy heights ranging from 0.2 to 1.8 m (estimated fraction of ground canopy cover was from 39 % up to 97 %). The land surface temperature (retrieved from Landsat 5 and 7) was used to partition soil and canopy temperatures. The eddy covariance (EC) method and the surface energy balance closure using the Bowen ratio (BR) method (estimated using the EC method) they both were taken as a reference. Regardless of the reference and crop, the results (linear regression analysis, the RMSE and the index of agreement, AI) obtained were comparable, or slightly better using the SR methodology (the AI ranged between 92 % (soybeans using the EC method) and 98 % (corn using the EC method) for SR and 83 % and 94 % (soybeans and corn, respectively, both using BR method) for the original method).

Abbreviation list and the input required to determine the sensible heat and the latent heat fluxes

Variable / Input required:	Symbols	Units	Meaning
Estimated	α	(-)	Parameter that corrects for the non-uniform scalar mixing within the parcel of air
Estimated / Yes	α_{PT}	(-)	Parameter that corrects for the evapotranspiration
Derived	β	(-)	The shape-parameter of the gamma function
Derived / Yes	γ	Pa K^{-1}	Psychrometric constant
Estimated / Yes	λ	(-)	Semi-empirical coefficient
Estimated / Yes	λ_v	(-)	Semi-empirical coefficient
Derived	ϕ_h	(-)	Flux-gradient stability function for heat transfer
Derived / Yes	ρ	kg m^{-3}	Density of air at reference height
Derived	τ	s	Ramp period determined using measurements taken at high frequency
Derived	τ_m	s	Exposure time for a fluid element
Derived / Yes	Δ	Pa K^{-1}	Slope of saturation vapor pressure curve at reference height
Derived	Ψ_m	(-)	Integrated stability function for momentum
Derived	Ω	(-)	Clumping factor
Derived	a_m	K	The net increment of temperature for a fluid element
Estimated / Yes	d	m	Zero-plane displacement
Measured / Yes	f_{row}	m	Width row
Measured	f_V	(-)	Vegetation fraction of soil
Constant / Yes	g	m s^{-2}	Gravity
Measured / Yes	h	m	Canopy height
Constant / Yes	k	(-)	von-Kármán constant
Measured / Yes	l	m	Leaf size

(*continued on next column*)

(*continued*)

(*continued on next page*)

* Corresponding author.
E-mail addresses: francesc.castellvi@udl.cat (F. Castellví), mariap.gonzalez.d@juntadeandalucia.es (M.P. González-Dugo).

https://doi.org/10.1016/j.agrformet.2025.110903
Received 30 April 2025; Received in revised form 15 October 2025; Accepted 17 October 2025
Available online 25 October 2025

(*continued*)

Variable / Input required:	Symbols	Units	Meaning
Measured / Yes	u	m s^{-1}	Horizontal mean wind speed at reference height
Derived	u_c	m s^{-1}	Horizontal mean wind speed at the canopy top
Derived	u_*	m s^{-1}	Friction velocity
Derived	y	(-)	Momentum exchange universal function for momentum
Estimated / Yes	z	m	Measurement height above d
Estimated / Yes	z_{0m}	m	Roughness length for momentum
Estimated / Yes	z_{0hS}	m	Roughness length for heat transfer for soil
Derived	A	K	Mean ramp amplitude for the temperature of the air
Derived	A_s	K	Mean ramp amplitude for the temperature of the air in contact with the soil
Derived	A_v	K	Mean ramp amplitude for the temperature of the air in contact with the vegetation
Derived / Yes	C	(-)	Parameter
Derived / Yes	C_p	J kg^{-1} K^{-1}	Isobaric heat capacity of air
	H	W m^{-2}	Actual sensible heat flux
Measured	H_{BR}	W m^{-2}	H using the Bowen ratio method
Measured	H_{EC}	W m^{-2}	H using the EC method
Derived	$H_{estimates}$	W m^{-2}	H using the SR_TS or KN1999 methods
Derived	H_{KN1999}	W m^{-2}	H using the KN1999 method
Derived	H_S	W m^{-2}	Soil sensible heat flux
Derived	H_{SR}	W m^{-2}	H using SR analysis
Derived	$H_{SR-T_{LS}}$	W m^{-2}	H using the $SR - T_{LS}$method
Derived	H_v	W m^{-2}	Vegetation sensible heat flux
Derived	L	m	Obukhov length
Derived	L_s	m	Shear-scale at the canopy top
Derived / Yes	LAI	m^2 m^{-2}	Leaf area index
	LE	W m^{-2}	Actual latent heat flux
Derived	LE_{EC}	W m^{-2}	LE using the EC method
Derived	LE_S	W m^{-2}	Soil latent heat flux
Derived	LE_v	W m^{-2}	Vegetation latent heat flux
Measured / Yes	T_{LS}	K	Land Surface Temperature
Measured	R_n	W m^{-2}	Net radiation
Derived / Yes	R_{ns}	W m^{-2}	Soil net radiation
Derived / Yes	R_{nv}	W m^{-2}	Vegetation net radiation
Measured / Yes	T	K	Air temperature at reference height
Derived / Yes	T_{AV}	K	Base - temperature of the ramp-like event
Derived / Yes	T_{ref}	K	Temperature of the air for sparse canopy at (Z_{0m}+ d)
Derived / Yes	T_s	K	Soil temperature
Derived / Yes	T_v	K	Vegetation temperature
Measured / Yes	Z	m	Measurement height above the ground taken as a reference
Estimated	Z_m^*	m	Roughness sub-layer depth for momentum
Estimated	Z_h^*	m	Roughness sub-layer depth for heat

1. Introduction

Many eco-hydrological studies rely on a simplified surface energy balance theory, which includes the net radiation (R_n), the soil heat flux (G), the latent heat flux (LE), and the sensible heat flux (H), as $R_n - G = H + LE$. For sparse vegetation, the key point is to partition radiation into latent heat flux and sensible heat flux (Shuttleworth and Wallace, 1985; Anderson et al., 2024). The portion of soil may represent an important source (or sink) of energy, implying that soil evaporation is non-negligible compared with plant transpiration and, therefore, is a key point to partition LE into evaporation and transpiration. This is of interest for agriculture to help water management decisions in water-scarce environments to improve yields, irrigation efficiency, and plant growth (Kool et al., 2014 and 2021; Anderson et al., 2017 and 2024). The Two-Source Energy Balance (TSEB) model is widely used for assessing these issues because it considers the soil and the vegetation canopy as separate sources.

The original TSEB, based on the Monin-Obukhov Similarity Theory (MOST) bulk transfer formulation (Brutsaert, 1982; Crago et al., 2014), was used for estimating ET by solving soil and plant energy balances using as input the land surface temperature, standard meteorological data, leaf area index, and a few site-specific parameters (Norman et al., 1995; Kustas and Norman, 1999; Sánchez et al., 2019). While ET estimates appear reasonable, their components (evaluated over different crops) showed that the accuracy appears dependent on season and the water-stressed conditions (Colaizzi et al., 2014; Song et al., 2015; Diarra et al., 2017; Santos, 2018; Kustas et al., 2018, among others), and recent advancements of the TSEB model have centered in (1) soil heat flux modelling, (2) plant transpiration parameterization and the net radiation captured by the plant canopy and (3) the partitioning of surface temperature into soil and plant canopy temperature components (Song et al., 2015; Colaizzi et al., 2016; Nieto et al., 2019; Parry et al., 2019; Anderson et al., 2024). However, the development of a TSEB-Lagrangian model in the framework of the Surface Renewal (SR) theory and its comparison is pending research. Here, SR replaces MOST in the TSEB series scheme to estimate the sensible heat flux while preserving standard TSEB inputs and remote-sensing compatibility. When MOST assumptions can be strained, SR within TSEB may be advantageous. The comparison with the original model (namely, KN1999's model, Kustas and Norman (1999)) was made using a dataset containing two contrasting crops, corn and soybeans. This well-documented and accessible dataset (Kustas et al., 2005) provides a wide range of canopy structures and crop phenology, including partial canopy coverage measured under varying soil moisture conditions and with sufficient footprints, making it especially useful for studying land-atmosphere energy exchanges.

For assessing the estimation of turbulent fluxes and water management irrigation, the earlier SR studies were focused on the one-source model mainly using high-frequency data (Paw et al., 1995; Castellví, 2004; French et al., 2012; Hu et al., 2018; Masanganise et al., 2022; among others), and a very few used low–frequency data (Castellví and Gonzalez-Dugo, 2021). Here, the purpose was to develop a hybrid SR-TSEB model to estimate sensible heat flux half-hourly using the same input requirements as the original. The application of satellite-derived land surface temperature opens new opportunities to upscale the SR method, complementing existing approaches and strengthening the remote sensing and hybrid modelling of ET.

In Section 2, Subsection 2.1 briefly introduces how the latent heat flux and the sensible heat flux are partitioned. Continuing with the sensible heat flux estimates, for homogenous surfaces (i.e, one source model), the subsection 2.1.1 introduces general concepts on the SR process, and subsections 2.1.2 and 2.1.3 describes how to estimate the sensible heat flux in the inertial sublayer and bare soil, respectively. For a sparse canopy (i.e., two-source model), Section 2.2 provides a scheme for modelling the continuity of the sensible heat fluxes and the temperatures involved and the section 2.3 gives a summary. The section 3 describes the main details of the experiments and the references used for comparison. In addition, how the estimations on soybean and maize under clear-sky and unstable conditions are validated. Section 4 shows the good performance of the hybrid SR-TSEB model indicating the future research pending and Section 5 concludes that it is an alternative to take into account.

2. Theory

2.1. Background

Knowing the time, the solar zenith angle and the standard meteorological variables, the soil heat flux, the net radiation and the radiation extinction parameter, the soil and the vegetation net radiation, R_{ns} and R_{nv}, respectively, can be estimated (Kustas and Norman, 1999). The land surface viewed from the nadir is composed of soil (s) and vegetation (v). Thus, the land surface temperature (T_{LS}), the soil temperature (T_s) and the vegetation temperature (T_v) are related with the vegetation fraction

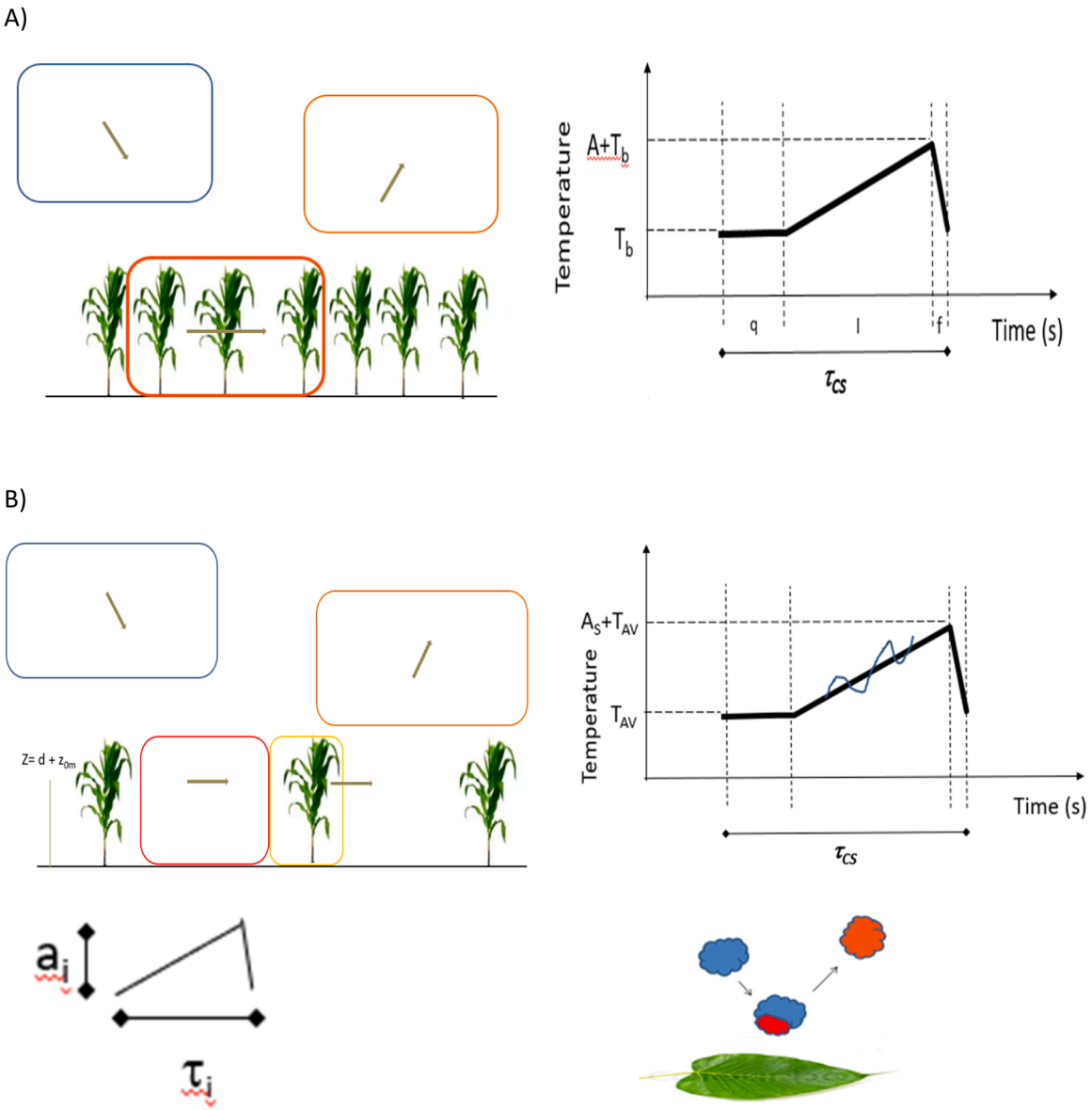

Fig. 1. Surface renewal (SR) scheme for an unstable case. A) From a lagrangian point of view (gray arrows denotes the motion of the parcel of air), taking measurements of the temperature of the air at the canopy top SR analysis focused on the role of a coherent structure (*CS*) (left), through the determination of the ramp period (τ_{CS}) and amplitude (A_{CS}) (right). After a quiescent period (q), the macro-parcel of air (orange) is heated during a period (l) until, by continuity, it is replaced during a period (f) (brown) by a cooler parcel (blue) coming from above with a mean temperature T_b (right), representing the signature of the *CS*. B) Taking measurements of the temperature of the air at the height, $Z = d + z_{0m}$ (d is the zero-plane displacement and z_{0m} is the roughness length for the momentum of the vegetation) (up left), with an initial temperature T_{AV} (quiescent period) the macro-parcel of air will be split into two sub-parcels of air (i.e., during the period τ_{CS} the warming of the macro-parcel of air was not homogeneous). One reaches the vegetation temperature (yellow), T_V, with an amplitude A_V and the other reaches the soil temperature (red), T_S, with an amplitude A_S. Considering the sub-parcel of air in contact with the vegetation (up right), the temperature trace (thick solid line) shows small fluctuations embedded in the sub-parcel signature (thin solid line). A small fluctuation follows a ramp-like shape (where the period q is neglected) and represents the signature of a fluid element (bottom left). The fluid element (blue) descents to the leaf (bottom right), and it is heated during τ_i (red) and replaced by another fluid element. The rapid turbulence mixing makes the temperature homogeneous (orange).

(f_V). The T_{LS} partitioning (Anderson et al., 2005)

$$T_{LS}^4 = (1 - f_v) T_s^4 + f_v T_v^4, \quad (1)$$

may be estimated through the leaf area index (LAI) and the clumping factor (Ω)

$$f_v = 1 - e^{-0.5\ LAI\ \Omega}, \quad (2)$$

or with the width row (f_{row}) being

$$(-0.5\ LAI\ \Omega) = \ln(1 - f_{row}) + f_{row}\ e^{-0.5\ LAI\ /f_{row}} \quad (3)$$

In the subsection 2.2.4 it is explained how to estimate the soil and the vegetation temperatures. The latent heat flux and the sensible heat flux can be partitioned as:

$$LE = LE_s + LE_v \quad (4)$$

$$H = H_s + H_v \quad (5)$$

Assuming no-advection and that the fraction of green vegetation is 1, LE_v is estimated using the Priestley–Taylor equation

$$LE_v = \alpha_{PT} \frac{\Delta}{\Delta + \gamma} R_{nv} \quad (6)$$

where α_{PT} is normally taken as 1.26 (potential value), Δ is the rate of change of saturated vapor pressure with air temperature and γ is the psychrometric constant (Priestley and Taylor, 1972). Given that R_{nv} and LE_v were estimated, it follows that H_v can be estimated, $R_{nv} = H_v + LE_v$. The next section shows how to estimate H and H_s using SR concepts.

In the following, the subsections 2.1.1, 2.1.2 and 2.1.3 summarized the One Source model for estimating the sensible heat flux based in SR analysis.

2.1.1. Surface renewal process

Regardless of the measurement height above the canopy, assuming a homogeneous surface for an unstable thermal stratification of the atmospheric surface layer, Fig. 1A shows an ideal comprehensive scheme for the SR process for estimating the sensible heat flux. Initially, it was assumed that a descending macro-parcel of air following a coherent motion remains in contact with the surface for a period (τ). A macro-parcel of air is a parcel whose volume covers all the sources. After a quiescent period, the macro-parcel of air is warmed while remaining in contact with the surface. By continuity, another *fresh* macro-parcel of air sweeps into the surface, replacing the previous one, which represents an injection of sensible heat into upper air layers. Thus, taking the temperature measured at the canopy top and sampling at a high frequency is possible to observe the peak and the sudden temperature drop corresponding to the ejection – sweep of the macro-parcel of air. The latter resembles the traces of a ramp-like event with amplitude A which, with τ together, represents the *signature* of the macro parcel (Van Atta, 1977; Paw et al., 1995; Katul et al., 1996; Chen et al., 1997a).

Assuming regular injections, the net enrichment of sensible heat can be determined as (Paw et al., 1995):

$$H_{SR} = rCpaZA/t \tag{7}$$

where ρ and C_p are the density and isobaric heat capacity of the air, respectively, (αZ) represents the volume per unit surface of the macro-parcel ejected, α is an empirical coefficient and Z is the measurement height (at the canopy top).

2.1.2. Estimating the sensible heat flux in the inertial sublayer

To apply Eq. (7) it is necessary to estimate the volume per unit surface of the macro-parcel ejected. In the inertial sublayer, combining MOST and SR concepts the following relationship was derived (Castellví, 2004; Fisher et al., 2023):

$$H_{SR} = \rho C_p \sqrt{\frac{kz\, u_* \, \varphi_{h(z/L)}^{-1}}{\pi\tau}} A, \tag{8}$$

where k is the Von Kármán constant ($k = 0.4$), z is the measurement height above the zero-plane displacement (d), $z = Z - d$, u_* is the friction velocity, $\phi_{h(z/L)}$ is the stability correction function for heat transfer, L is the Obukhov length, $L = -\frac{u_*^3}{kgH}\rho C_p T$. T is the temperature of the air and g is the gravitational acceleration rate.

Equation (8) was applied using half-hourly values, $H_{SR-T_{LS}}$ (Castellví et al., 2014, 2016; Castellví and Oliphant, 2017; Castellví and González-Dugo, 2021):

$$H_{SR-T_{LS}} = \rho C_p \left(\frac{4k}{\pi\lambda}\right)^{\frac{1}{2}} \frac{\left(z\hbar\phi_h^{-1}\left(\frac{z}{L}\right)\right)^{\frac{1}{2}} ku_*}{Z\left(\ln\frac{z}{z_{0m}} + 2\right)} (LST - T), \tag{9}$$

where the coefficient λ (defined as $\lambda = \frac{z}{\tau u_*}$ (Chen et al., 1997b)) was set to 0.5 for unstable cases, h is the canopy height, z_{0m} is the surface roughness length for momentum evaluated at neutral conditions, $z_{0m} = 0.12\ h$ (Brutsaert, 1982) and $\phi_{h(z/L)}$ is (Dyer, 1974);

$$\varphi_{h(z/L)} = \left(1 - 16\frac{z}{L}\right)^{-1/2} \tag{10}$$

The wind log-law was used to estimate the friction velocity from the horizontal mean wind speed measured at the reference height (u)

$$u_* = \frac{ku}{\ln\frac{z}{z_{0m}} - \Psi_{m(z/L)} + \Psi_{m(z_{0m}/L)}} \tag{11}$$

and $\Psi_{m\ (z/L)}$ and $\Psi_{m\ (z0m/L)}$ are the integrated stability function for momentum transfer determined at z/L and z_{0m}/L, respectively. For unstable cases (Brutsaert, 1982);

$$\Psi_{m(z/L)} = 2\ln\left(\frac{1+y}{2}\right) + \ln\left(\frac{1+y^2}{2}\right) - 2\arctan y + \frac{\pi}{2} \tag{12}$$

with

$$y = (1 - 16\ z/L)^{0.25} \tag{13}$$

2.1.3. Estimating the sensible heat flux from the soil

Assuming the ground is composed of bare soil, starting from Eq. (8), the following expression was derived for estimating the sensible heat flux under unstable cases (Castellví and Agam, 2025):

$$H_s = \rho C_p \left(\frac{k}{\pi}\frac{C}{0.31}\left(\frac{gz_{0h_s}}{T_{ref}}\right)^{1/3} u\right)^{3/5} \left(\frac{T_s - T_{ref}}{\ln\frac{Z}{z_{0h_s}}}\right)^{6/5}, \tag{14}$$

where T_S is the temperature of the soil, T_{ref} is a reference temperature of the air and z_{0h_s} is the surface roughness length for heat transfer evaluated at neutral conditions, $z_{0h_s} = z_{0ms}e^{-2}$ (Crago and Qualls, 2014) and z_{0ms} is the surface roughness length for momentum at the ground. The parameter C is a non-dimensional relationship defined as, $\frac{1}{\lambda}\left(\frac{k}{\alpha}\right)^2\left(\frac{kz}{z_{0h_s}}\right)^{1/3}\left(\frac{u_*}{u}\right) = C$, where C was 0.5 and it performed fairly constant versus height for different bare soils (Castellví and Agam, 2025).

2.2. The two – source model

In this section, an ideal scheme for the continuity of the sensible heat fluxes and their temperatures involved in a sparse canopy at the height $Z = (z_{0m} + d)$ is proposed.

2.2.1. The roughness sublayer. From the ground to the canopy height

In this sublayer, the warming of the macro-parcel of air is not homogeneous, and depends on the temperature of the soil and the vegetation. The macro-parcel of air will be split into two sub-parcels. The mean net temperature increase for the macro sub-parcels in contact with the soil and the vegetation during τ will be denoted by A_s and A_v, respectively.

The SR process is idealized as shown in Fig. 1B. When the descending macro-parcel of air is close to the surface it cannot absorb all the momentum transferred to the ground and a new population of small eddies (namely fluid elements) are generated within each macro sub-parcels. The fluid elements are presumed randomly distributed and remain attached to their corresponding macro sub-parcel of air. During the time that a fluid element remains close to the viscous boundary layer adjacent to a source, τ_m (exposure time), fluxes transfer through the interface and, therefore, the fluid element increases its temperature, a_m, until it is randomly replaced by another fluid element (Danckwerts, 1951; Harriot et al., 1962). At a given measurement height, the actual time series of the temperature of the air shows small fluctuations embedded in their corresponding macro sub-parcel. The latter fluctuations in the temperature trace is the *signature* of a fluid element attached to the macro sub-parcel of air which will be assumed to follow a ramp-like shape characterized

by a gradual increase of the temperature (warming phase) followed by a sudden drop in temperature (Fig. 1B). The latter indicate that this fluid element was replaced by another cooler fluid element. Taking the temperature sampled at a high frequency, the signature of a fluid element can be estimated by the time difference observed between two consecutive valleys (τ_m) and by an amplitude, which is the temperature difference between the peak and the earlier valley (a_m) (Fig. 1B) (Castellví, 2018). Considering the macro sub-parcel of air remaining in contact with the vegetation, integrating the amplitudes of the fluid elements leads to;

$$A_v = \frac{1}{\overline{\tau}_m}\sum_{1}^{N_v} a_m \tau_m, \tag{15}$$

where N_v is the number of fluid elements in the vegetation. Similarly, for the ground;

$$A_s = \frac{1}{\overline{\tau}_m}\sum_{1}^{N_s} a_m \tau_m \tag{16}$$

N_s denotes the number of fluid elements at the ground. Therefore, measuring the temperature traces at $Z = (z_{0m} + d)$, the ramp amplitude of the macro sub-parcel of air remaining in contact with the vegetation and for the ground will be, respectively,

$$A_v = T_V - T_{AV} \tag{17}$$

$$A_s = T_s - T_{AV} \tag{18}$$

where T_{AV} is the base - temperature of the ramp-like event (i.e., the quiescent period). Thus, in the context of Eq. (14) it will be assumed that T_{ref} is T_{AV}.

2.2.2. The roughness sublayer. Above the canopy height

When a *fresh* macro-parcel of air descends to the ground to renew the previous one, the above-mentioned fluid elements will be ejected upwards attached to their corresponding macro sub-parcel of air. Above the canopy, turbulence rapidly mixes the air of the two macro sub-parcels of air, therefore, giving a unique probability distribution function for the ramp period of fluid elements (Zhu et al., 2007). For the horizontal velocity traces, the probability distribution function (PDF) of the exposure time can be described as:

$$PDF_{(\tau_m)} = \frac{(\beta+1)^{(\beta+1)}}{\Gamma_{(\beta+1)}}\frac{\tau_m^{\beta}}{\overline{\tau}_m^{(\beta+1)}} e^{-\left((\beta+1)\frac{\tau_m}{\overline{\tau}_m}\right)}, \tag{19}$$

where Γ is the gamma function, $\overline{\tau_m}$ is the mean of exposure time of fluid elements population and β is a shape-parameter (Bullin and Dukler, 1972; Seo and Lee, 1988). For fluctuations in the temperature of the air (determined as the time difference between two consecutive peak and valley observed in the temperature traces) the probability distribution function of the exposure time can be described by Eq. (19) and it was shown that the corresponding β parameter allows for estimating the friction velocity (Castellví, 2018; Castellví et al., 2020a, b and 2021):

$$u_* = \begin{cases} \dfrac{k u}{\beta}\phi^{-1}_{m\left(\frac{Z-d}{L}\right)} & Z-d \geq (h-d)\left[\dfrac{3+ln(\beta)}{ln(\beta)}\right] \ (inertial) \\ \dfrac{k u}{\beta}\dfrac{(h-d)}{(Z-d)}\left[\dfrac{3+ln(\beta)}{ln(\beta)}\right]\phi^{-1}_{m\left(\frac{Z-d}{L}\right)} & Z-d < (h-d)\left[\dfrac{3+ln(\beta)}{ln(\beta)}\right] \ (roughness) \end{cases} \tag{20}$$

2.2.3. The top of the roughness sublayer

The roughness sub-layer depth for momentum (Z_m^*) and heat (Z_h^*) can be estimated, respectively, as (Raupach et al., 1996; Mölder et al., 1999; Leclerc and Foken, 2014):

$$\left(Z_m^* - d\right) = (h-d) + 2L_s \text{ and } \left(Z^*{}_h - d\right) = (h-d) + 3L_s, \tag{21}$$

where L_s is the shear-scale, $L_s = \frac{u}{d\psi/dz}$ evaluated at h (Raupach et al., 1996). At near-neutral conditions, L_s can be approached to; $\frac{1}{L_s} = \frac{ln(\beta_{Z=h})}{(h_c-d)}$ (Castellví, 2018). Above the canopy the roughness sub-layer is mostly coherent (Raupach et al., 1996), thus by invoking coherency (i.e., from the canopy top up to the roughness sub-layer) it will be assumed that the shape-parameter β will remain fairly constant

$$L_s = \frac{(h-d)}{\ln\beta}, \tag{22}$$

with β measured at any height within the roughness sub-layer. For field applications, Eq. (22) was roughly assumed valid for unstable conditions and combining Eqs. (21) – (22) the top of the roughness sub-layer for momentum and heat can be estimated as:

$$\left(Z_m^* - d\right) = (h-d)\frac{(\ln\beta + 2)}{\ln\beta} \text{ and } \left(Z^*{}_h - d\right) = (h-d)\frac{(\ln\beta + 3)}{\ln\beta} \tag{23}$$

The wind log-law evaluated at the top of the roughness sub-layer for momentum can be expressed as, $u_{Z_m^*} - \frac{u_*}{k}\left[\ln\frac{z}{z_{0m}} - \Psi_{m\left(z_m^*/L\right)} + \Psi_{m\left(z_{0m}/L\right)}\right] = 0$. The latter, combined with Eq. (20) and (23) and invoking coherency in the roughness sub-layer leads to:

$$\beta\varphi_{m\left(z_m^*/L\right)} - \ln\left[\left(\frac{h-d}{z_{0m}}\right)\left(\frac{2+\ln\beta}{\ln\beta}\right)\right] - \Psi_{m\left(z_m^*/L\right)} + \Psi_{m\left(z_{0m}/L\right)} = 0, \tag{24}$$

which allows estimating βas follows. Starting at neutral conditions, a first approach for $\beta$is determined. Next, using the Obukhov length (determined from $H_{SR-T_{LS}}$, Eq. (9)) the first approximation of the stability parameter is obtained (using Eqs. 23 - 24), which allows estimating a new value ofβ. Therefore, using u_* (determined from the wind log-law), the wind speed at the canopy top can be estimated using Eq. (20).

2.2.4. Estimating T_V, T_s and T_{AV}

Given that the vegetation sensible heat flux was estimated, the vegetation temperature can be retrieved via Eq. (9):

$$H_v = \rho C_p\left(\frac{4k}{\pi\lambda}\right)^{1/2}\frac{\left(zh\phi_{h(z/L)}^{-1}\right)^{1/2}ku_*}{Z\left(\ln\frac{z}{z_{0m}} + 2\right)}(T_v - T) \quad , \tag{25}$$

allowing estimating the soil temperature from ${T_{LS}}^4 = (1-f_v){T_s}^4 + f_v\,{T_v}^4$ (Anderson et al., 2005). In a SR experiment taking measurements within the canopy it was found that the sensible heat flux measured at the height $Z = (d + z_{0m})$ can be estimated from Eq. (7) setting $\alpha = 1$ (Spano et al., 2000):

$$H_V = \rho C_p(d + z_{0m})\frac{A_v}{\tau} \tag{26}$$

When the macro parcel of air descends to the ground, it will follow a horizontal motion (Fig. 1B) and the initial temperature at height $Z = (d + z_{0m})$ is T_{AV} (quiescent period). After the warming period, it finally will be T_V, thus the ramp amplitude is, $A_V = T_V - T_{AV}$. Based on Chen et al. (1997b), here it is assumed that the ramp period can be estimated as, $\frac{1}{\tau} = \lambda_v\frac{u_{*(d+z_{0m})}}{(d+z_{0m})}$ with λ_v an empirical coefficient, thus Eq. (26) was rewritten:

$$H_V = \rho C_p\lambda_v(T_V - T_{AV})\frac{u_{*(d+z_{0m})}}{(d+z_{0m})} \tag{27}$$

Assuming near neutral conditions and using the relationship $u_{*(d+z_{0m})} = \frac{k\,u}{\beta}$, it was found that a representative value for lnβ was 0.75

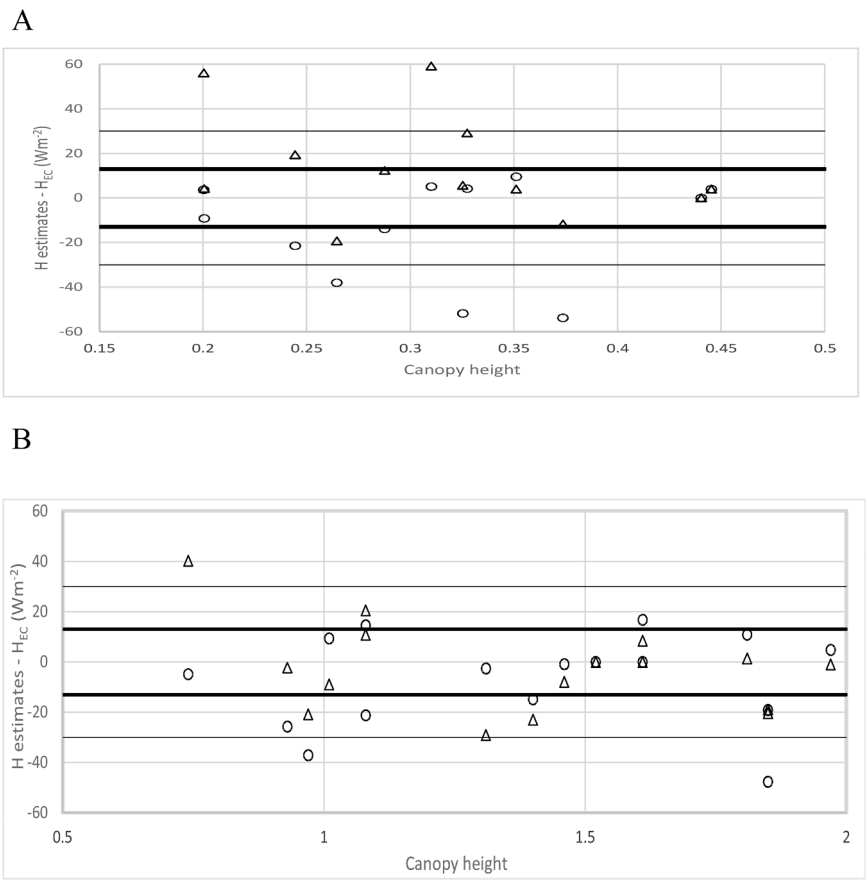

Fig. 2. Instantaneous sensible heat flux errors ($H_{estimates} - H_{EC}$) versus the canopy height for soybean (A) and corn (B). The $H_{estimates}$ were determined using methods H_{SR_TS} (triangles) and H_{KN1999} (circles). The solid lines ± 13 Wm^{-2} denote the EC uncertainty and ±30 Wm^{-2} denote the measurement error in estimating the sensible heat flux.

(Castellví, 2018), thus:

$$u_* = ke^{-0.75}\mathrm{u} \tag{28}$$

The wind velocity at $Z = (d + z_{0m})$ can be estimated as (Goudriaan, 1977)

$$u = u_c \exp\left(-0.28\, LAI^{\frac{2}{3}} h^{\frac{1}{3}} l^{-\frac{1}{3}}\left(1 - \frac{(d + z_{0m})}{h}\right)\right), \tag{29}$$

where l is the leaf size (i.e., l is given by the four times the leaf area divided by the perimeter). Here, as a rule of thumb, it was proposed to set $\lambda_v = 0.5$. Therefore, T_{AV} can be rearranged (i.e., combining Eqs. ($R_{nv} = H_v + LE_v$), (20) (evaluated at the canopy top), (27) and (28)).

2.3. Summary of the new concept

The SR-TSEB hybrid method proposes a model for estimation of the sensible heat flux using SR and MOST concepts for sparse canopies, the other modelled energy fluxes (Rn, G and LE) remained the same as proposed in the KN1999 model. SR is inserted at the sensible-heat flux step within the series scheme. The sensible heat flux estimation requires expressions based in low-frequency (half-hourly) measurements. Initially, during the incursion of the macro-parcel of air (covering all the heat sources; soil and vegetation up to canopy top) is assumed to have a uniform temperature (T_{AV}). After a quiescent period, the different warming is modelled assuming that the macro-parcel of air was split into two sub-parcels of air (Fig. 1B). One has the temperature net increase of the soil, $A_s = T_s - T_{AV}$, and the other the temperature net increase of the vegetation, $A_V = T_V - T_{AV}$. Afterwards, the two sub-parcels of air ejected up to the inertial layer. When they are both above the canopy height (in the roughness sub-layer), turbulence rapidly mixed the air of the two macro sub-parcels of air. A scheme to link the continuity of the variables (such as the wind, the temperatures and the sensible heat flux) from the point $Z = (d + z_{0m})$ up to the inertial sub-layer is able to estimate separately the temperatures T_s, T_V and T_{AV}, and, therefore, the H_v and H_s.

3. Experimental data

The ground dataset used in this study is part of the Soil Moisture–Atmosphere Coupling Experiment (SMACEX) campaign, described in Kustas et al., 2005. This comprehensive dataset includes measurements of surface energy, water, and carbon fluxes, as well as the collection of remote sensing imagery. The campaign was conducted alongside the Soil Moisture Experiment 2002 (SMEX02) at the Walnut Creek Watershed in central Iowa, from June 20 to July 9, 2002. SMEX02 provided valuable spatially and temporally distributed information of canopy properties, such as crop height and leaf area, which critically influence surface roughness and flux modelling. Ground flux measurements were collected at 12 fields, 6 grown with corn and 6 with soybeans. For additional details of the combined SMACEX-SMEX02 field campaigns see Kustas et al. (2003).

The turbulent fluxes were measured using the Eddy Covariance (EC) method. For each field, the EC instrumentation was deployed at about two times the canopy height, and no flux divergence was observed. The 20-Hz data were first despiked to remove anomalies in the main fluxes and micrometeorological variables, passed through a low-frequency filter, and then used to compute the 30-min averages. Additionally, a

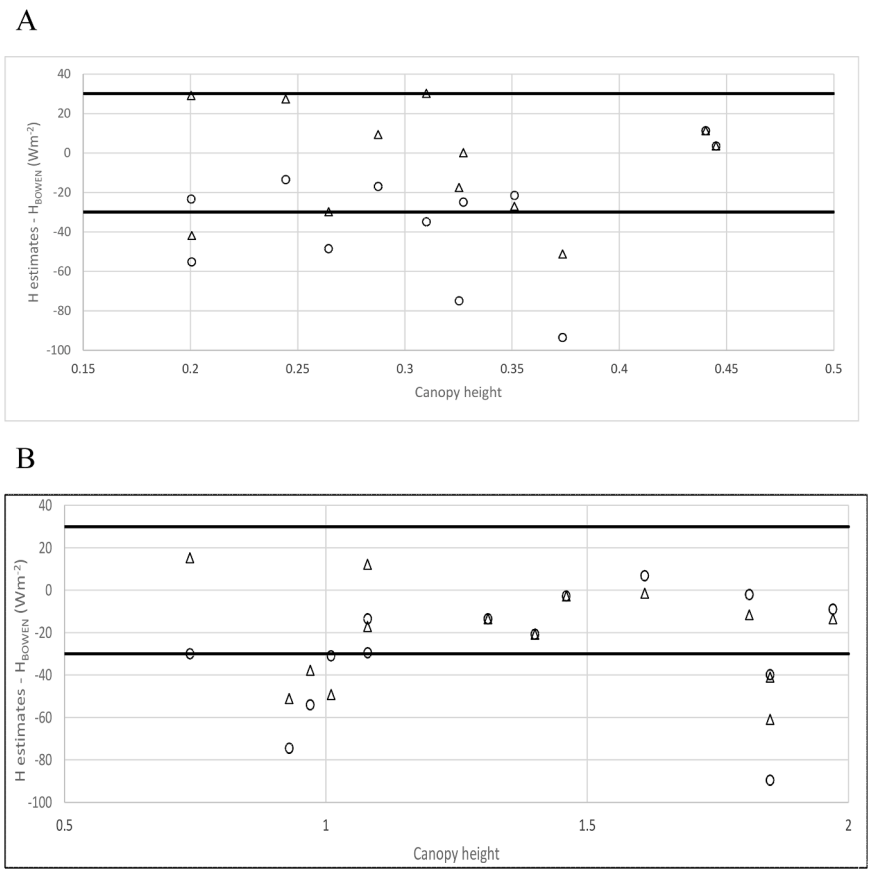

Fig. 3. Instantaneous sensible heat flux errors ($H_{estimates} - H_{BOWEN}$) versus the canopy height for soybean (A) and corn (B). The $H_{estimates}$ were determined using methods H_{SR_TS} (triangles) and H_{KN1999} (circles). The solid lines ($\pm$30 Wm^{-2}) denote the measurement error in estimating the sensible heat flux.

two-dimensional coordinate rotation and corrections for heat density effects were applied to the scalar fluxes. Further outlier control was performed on the 30-minute fluxes considering daily trends. This process was completed for each tower, resulting in a data capture during the study of greater than 95 %. Ancillary measurements included energy balance components, net radiation, and soil surface heat flux, achieving an energy balance closure of about 85 % (Prueger et al., 2005).

The operational towers for the days and times relevant to this study correspond to those described by Gonzalez-Dugo et al. (2009). For comparison purposes, the 30-min fluxes measured during satellite overpasses (between 10:29 and 10:48 CST, depending on the date and the sensor) were selected.

The surface energy balance closure of the measurements was forced using both the Bowen ratio method and the residual-LE closure method. The first method assumes that the Bowen ratio is correctly measured using the EC method (Twine et al., 2000). The residual-LE closure method relies on accurate measurements of H. Here, it was considered irrelevant to investigate which of the two could be the best (Zhou et al., 2023), so both were used as a reference.

Land surface temperature data were obtained from the Landsat 5 Thematic Mapper (TM) and Landsat 7 Enhanced Thematic Mapper Plus (ETM+), processed as described by Gonzalez-Dugo et al. (2009).

4. Results and discussion

In the following, the TS model estimated using the SR will be referred to SR_TS. The Figs. 2 and 3 show the instantaneous errors ($H_{estimated} - H_{EC}$) and ($H_{estimated} - H_{Bowen}$), respectively, obtained for SR_TS and HKN1999 versus the canopy height. Fig. 2 included the thresholds of $\pm$ 13 W m^{-2} which represents the EC uncertainty (Mauder et al., 2007). Figs. 2 and 3 included $\pm$ 30 W m^{-2} thresholds representing the typical maximum error in estimating the sensible heat flux in flat and uniform terrain (Foken, 2008). For soybean, Fig. 2A shows that SR_TS and HKN1999 performed rather similar, both giving 7 samples (out of 12) in agreement with to the EC method. The SR_TS did two samples and the HKN1999 did three samples outside the thresholds of $\pm$ 30 W m^{-2} . For corn (Fig. 2B), SR_TS and HKN1999 performed similarly, giving 9 versus 8 samples (out of) in agreement with to the EC method. The SR_TS did one sample and HKN1999 did two samples outside the thresholds of $\pm$ 30 W m^{-2}, respectively.

Table 1
H_{SR_TS} and H_{KN1999} versus the reference (H_{EC} and H_{BR}). The number of data were 12 and 14 for soybean and corn, respectively. Int denotes the intercept of the linear regression analysis and the RMSE is the root mean square error (units W m^{-2}) and IA is the index of agreement.

Crop	Model	EC:	BOWEN:								
		Slope	Int.	R2	RMSE	IA	Slope	Int.	R2	RMSE	IA
Soybean	H_{SR_TS}	1.03	12	0.95	30	0.92	0.92	5	0.89	28	0.94
	H_{KN1999}	0.73	3	0.90	27	0.92	0.65	16	0.89	46	0.83
Corn	H_{SR_TS}	1.00	-2	0.93	19	0.98	0.76	1	0.89	31	0.96
	H_{KN1999}	0.69	13	0.89	21	0.91	0.55	11	0.87	39	0.94

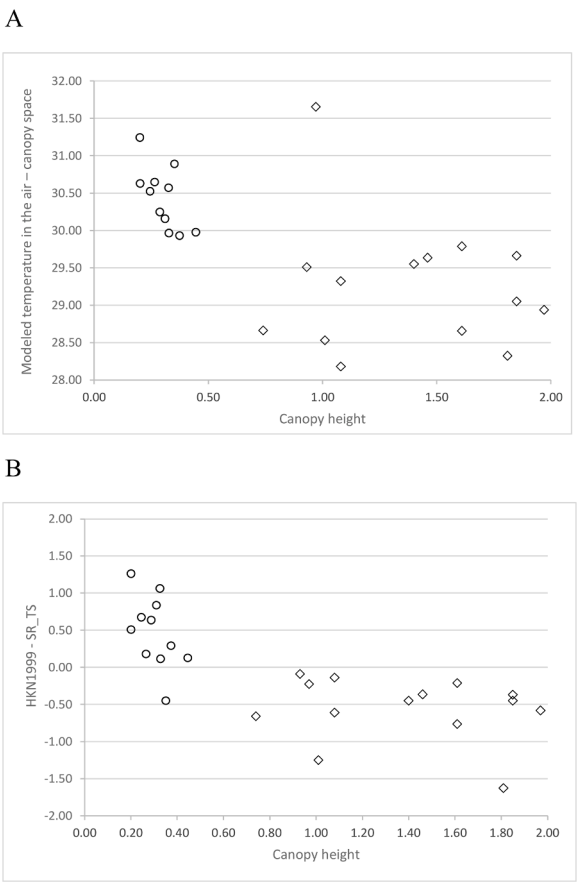

Fig. 4. A) The temperature modeled in the air – canopy space using the original (KN1999) and B) the instantaneous difference of the temperature, (KN1999 - SR_TS), versus the canopy height for corn (diamonds) and soybean (circle).

For soybeans, Fig. 3A shows that SR_TS did two samples and HKN1999 did five samples falling out respect ± 30 W m^{-2} thresholds. For corn (Fig. 3B), SR_TS did five samples and HKN1999 did four samples falling out respect ± 30 W m^{-2} thresholds. In general, both methods performed similarly with respect to EC Bowen ratio method.

Table 1 compares the H estimates against the references for each crop. Linear regression was used and the error metric was evaluated using the RMSE and the index of agreement (IA) (Willmott, 1981). The latter stands as a standardized metric for quantifying the degree of prediction error in models, bounded (between 0 and 1, with higher index values indicating that the modelled values have better agreement with the observations) and non-dimensional measure. The intercepts of the linear regression analysis were small, ranging between -2 and 16 W m^{-2}. For SR_TS the slopes were close to one (ranging between 0.92 and 1.05) except at corn using the Bowen ratio method that was 0.76. For HKN1999, the latter ranged between 0.55 and 0.73. The correlation for both methods was good, for SR_TS the R^2 ranged between 0.89 and 0.95 and for HKN1999 between 0.87 and 0.90. Regardless of the crop, the slopes and the coefficient of determination, R^2, were in general better for SR_TS than HKN1999. For SR_TS, regardless of the crop and the reference, the RMSE ranged in the interval 19 – 31 W m^{-2} and the IA between 92 % and 98 %, indicating that the performance was good. For HKN1999, the best results were obtained using the EC method; the RMSE were small (ranging between 21 W m^{-2} and 27 W m^{-2}) and the IA was good (ranging between 91 % and 92 %). Using the Bowen ratio method the RMSE were 46 W m^{-2} and 39 W m^{-2} for soybean and corn, respectively, and the IA were 83 % and 94 % for soybean and corn, respectively.

The SR_TS was comparable and even better than HKN1999 and, regardless of the crop and the reference, the Table 1 shows that its performance was similar indicating that potential differences between crops, such as LAI, crop architecture and field conditions, apparently were not relevant.

For each crop, Fig. 4A shows the modelled temperature in the air – canopy space at $Z = (d + z_{0m}z_{om})$ obtained by HKN1999 and, in Fig. 4B, shows their difference between models HKN1999 and SR_TS, (HKN1999 - SR_TS). Given that T_{AV} (determined by the SR_TS) corresponds to the quiescent temperature, (HKN1999 - SR_TS) was expected always positive. The expected performance was obtained for soybean, except for one case. However, the modeled (HKN1999 - SR_TS) values for corn were consistently negative. The different sign of (HKN1999 - SR_TS) may be the reason to under estimation the sensible heat flux. In fact, H_{SR_TS} tended to be closer to the references (Table 1) indicating that SR_TS modelling appears more reliable.

More research is pending, such as SR_TS performances for other crops and environmental conditions, how it could feature in future energy balance models, irrigation planning or remote sensing tools, the comparison versus the SR parallel model scheme and checking the ramp amplitudes for soil and canopy using high-frequency data.

5. Concluding remarks

We developed a two-source sensible heat flux model based on surface renewal theory. SR replaces MOST within the series-scheme TSEB while retaining inputs and remote-sensing compatibility. The model estimates the macro-parcel air temperature during the quiescent period at $d + z_{0m}$. The latter is the key for evaluating the maximum temperatures of the two sub-parcels of air in contact with the soil and the vegetation during the exposure, respectively. Taking as T_{AV} the ramp-temperature baseline, we estimate ramp amplitudes for soil and canopy as $A_s = T_s - T_{AV}$ and $A_v = T_V - T_{AV}$. The index of agreement for SR_TS was generally higher than that for HKN1999. Therefore, the estimated SR_TS sensible heat fluxes were comparable, or slightly better than, the original two-source model, supporting SR as an alternative to the MOST framework.

Funding

This work is part of the research project PID2021-124006OB-I00 funded by MCIN/AEI/10.13039/501100011033 and by the European Regional Development Fund (ERDF A way of making Europe).

Availability of data and materials

All the materials are free available.

Ethics approval and consent to participate

Not applicable.

Consent for publication

Not applicable.

CRediT authorship contribution statement

Francesc Castellví: Writing – review & editing, Writing – original draft, Software, Methodology, Conceptualization. **María P. González-Dugo:** Writing – review & editing, Software, Resources, Funding acquisition, Data curation.

Declaration of competing interest

The authors declare that they have no known competing financial interests or personal relationships that could have appeared to influence the work reported in this paper.

Acknowledgements

The authors acknowledge the referees for the review task. This work is part of the research project PID2021-124006OB-I00 funded by MCIN/AEI/10.13039/501100011033 and by the European Regional Development Fund (ERDF A way of making Europe) and it was supported under projects RTI2018-098693-B-C31 Ministerio de Ciencia, Economía y Universidades of Spain and the project PAGOSER-SAT with code PID2019-107693RR-C22 funded by MICIU/AEI /10.13039/501100011033. For data availability, contact María P. González-Dugo.

References

Anderson, M.C, Kustas, W.P, Norman, J.M, Diak, G.T, Hain, C.R, Gao, F., Yang, Y., Knipper, K.R, Xue, J., Yang, Y., Crow, W.T, Holmes, T.R.H, Nieto, H., Guzinski, R., Otkin, J.A, Mecikalski, J.R, Cammalleri, C., Torres-Rua, A.T, Zhan, X., Fang, L., Colaizzi, P.D, Agam, N., 2024. A brief history of the thermal IR-based two-source energy balance (TSEB) model – diagnosing evapotranspiration from plant to global scales. Agric. For. Meteorol. 350, 109951. https://doi.org/10.1016/j.agrformet.2024.109951.

Anderson, R.G., Zhang, X., Skaggs, T.H., 2017. Measurement and partitioning of evapotranspiration for application to vadose zone studies. Vadose Zo. J. 16. https://doi.org/10.2136/vzj2017.08.0155.

Anderson, M.C., Norman, J.M., Kustas, W.P., Li, F., Prueger, J.H., Mecikalski, J.R., 2005. Effects of vegetation clumping on two–source model estimates of surface energy fluxes from an agricultural landscape during SMACEX. J. Hydrometeorol 6, 892–909. https://doi.org/10.1175/JHM465.1.

Brutsaert, W., 1982. Evaporation into the Atmosphere. Environmental Fluid Mechanics. Kluwer Academic Publishers, Dordrecht/Boston/London, p. 299.

Bullin, J., Dukler, A.E., 1972. Random eddy models for surface renewal: Formulation as a stochastic process. Chem. Eng. Sci. 27 (2), 439–442. https://doi.org/10.1016/0009-2509(72)85081-4.

Castellví, F., Agam, N., 2025. A new approach to estimate the sensible heat flux in bare soils. Atmosphere 16, 3. https://doi.org/10.3390/atmos16040458.

Castellví, F., González-Dugo, M.P., 2021. A one - source model to estimate sensible heat flux in agricultural landscapes. Agric. For. Meteorol. 310, 135–144. https://doi.org/10.1016/j.agrformet.2021.108628.

Castellví, F., Medina, E., Cavero, J., 2020. Surface eddy fluxes and friction velocity estimates taking measurements at the canopy top. Agric. Water Manag. 241, 106358. https://doi.org/10.1016/j.agwat.2020.106358.

Castellví, F., Suvocarev, K., Reba, M.L., Runkle, B.R.K., 2020. Friction-velocity estimates using the trace of a scalar and the mean wind speed. Bound.-Layer Meteorol. 105–123. https://doi.org/10.1007/s10546-020-00520-1.

Castellví, F., 2018. An advanced method based on surface renewal theory to estimate the friction velocity and the surface heat flux. Water Resour. Res. 54. https://doi.org/10.1029/2018WR022808, 10,134-10,154.

Castellví, F., Oliphant, A.J., 2017. Daytime sensible and latent heat flux estimates for a mountain meadow using in-situ slow-response measurements. Agric. For. Meteorol. 236, 135–144. https://doi.org/10.1016/j.agrformet.2017.01.003.

Castellví, F., Cammalleri, C., Ciraolo, G., Maltese, A., Rossi, F., 2016. Daytime sensible heat flux estimation over heterogeneous surfaces using multi-temporal land-surface temperature observations. Water Resour. Res. 52, 3457–3476. https://doi.org/10.1002/2015WR017587.

Castellví, F., Gavilán, P., González-Dugo, M.P., 2014. Combining the bulk transfer formulation and surface renewal analysis for estimating the sensible heat flux without involving the parameter. Water Resour. Res. 50, 8179–8190. https://doi.org/10.1002/2013WR014950.

Castellví, F., 2004. Combining surface renewal analysis and similarity theory: A new approach for estimating sensible heat flux. Water Resour. Res. 40, W05201. https://doi.org/10.1029/2003WR002677.

Chen, W., Novak, M.D., Black, T.A., Lee, X., 1997a. Coherent eddies and temperature structure functions for three contrasting surfaces. Part I. Ramp model with finite micro-front time. Bound.-Layer Meteorol. 84, 99–123. https://doi.org/10.1023/A:1000338817250.

Chen, W., Novak, M.D., Black, T.A., Lee, X., 1997b. Coherent eddies and temperature structure functions for three contrasting surfaces. Part II. Renewal model for sensible heat flux. Bound.-Layer Meteorol. 84, 125–147. https://doi.org/10.1023/A:1000342918158.

Colaizzi, P.D., Agam, N., Tolk, J.A., Evett, S.R., Howell, T.A., O'Shaughnessy, S.A., Gowda, P.H., Kustas, W.P., Anderson, M.C., 2016. Advances in a two-source energy balance model: partitioning of evaporation and transpiration for cotton. Trans. ASABE 59, 181–197. https://doi.org/10.13031/trans.59.11215.

Colaizzi, P.D., Agam, N., Tolk, J.A., Evett, S.R., Howell, T.A., Gowda, P.H., O'Shaughnessy, S.A., Kustas, W.P., Anderson, M.C., 2014. Two-source energy balance model to calculate E, T, and ET: comparison of Priestley-Taylor and Penman-Monteith formulations and two time scaling methods. Trans. ASABE 57, 479–498. https://doi.org/10.13031/trans.57.10423.

Crago, R.D., Qualls, R.J., 2014. Use of land surface temperature to estimate surface energy fluxes: contributions of Wilfried Brutsaert and collaborators. Water Resour. Res. 50, 3396–3408. https://doi.org/10.1002/2013WR015223.

Danckwerts, P., 1951. Significance of liquid-film coefficients in gas absorption. Ind. Eng. Chem. 43 (6), 1460–1467. https://doi.org/10.1021/ie50498a055.

Diarra, A., Jarlan, L., Er-Raki, S., Le Page, M., Aouade, G., Tavernier, A., Boulet, G., Ezzahar, J., Merlin, O., Khabba, S., 2017. Performance of the two-source energy budget (TSEB) model for the monitoring of evapotranspiration over irrigated annual crops in North Africa. Agric. Water Manag. 193, 71–88. https://doi.org/10.1016/j.agwat.2017.08.007.

Dyer, A.J., 1974. A review of flux-profile relationships. Bound.-Layer Meteorol. 7, 363–372. https://doi.org/10.1007/BF00240838.

French, A., Alfieri, J., Kustas, W.P., Prueger, J., 2012. Estimation of surface energy fluxes using surface renewal and flux variance techniques over an advective irrigated agricultural site. Adv. Water Resour. 50. https://doi.org/10.1016/j.advwatres.2012.07.007.

Fisher, M., Katul, G.G., Noormets, A., Poznikova, G., Domec, J.C, Orság, M., Zalud, Z., Trnka, M., King, J.S., 2023. Merging flux-variance with surface renewal methods in the roughness sublayer and the atmospheric surface layer. Agric. For. Meteorol. 342, 109692. https://doi.org/10.1016/j.agrformet.2023.109692.

Foken, T., 2008. The energy balance closure problem: an overview. Ecol. Appl. 8 (6), 1351–1367. https://doi.org/10.1890/06-0922.1.

Gonzalez-Dugo, M.P., Neale, C.M.U., Mateos, L., Kustas, W.P., Prueger, J.H., Anderson, M.C., Li, F., 2009. A comparison of operational remote sensing-based models for estimating crop evapotranspiration. Agric. For. Meteorol. 149 (11), 1843–1853. https://doi.org/10.1016/j.agrformet.2009.06.012.

Goudriaan, J., 1977. Crop Micrometeorology: A Simulation Study (Simulation Monographs). Pudoc, Center for Agricultural Publishing and Documentation, Wageningen.

Harriott, P., 1962. A random eddy modification of the penetration theory. Chem. Eng. Sci. 17 (3), 149–154. https://doi.org/10.1016/0009-2509(62)80026-8.

Hu, Y., Buttar, N.A., Tanny, J., Snyder, R.L., Savage, M.J., Imran Ali Lakhiar, I.A., 2018. Surface renewal application for estimating evapotranspiration: A review. Adv. Meteorol. https://doi.org/10.1155/2018/1690714.

Katul, G.G., Hsieh, C-I., Oren, R., Ellsworth, D., Philips, N., 1996. Latent and sensible heat flux predictions from a uniform pine forest using surface renewal and flux variance methods. Bound.-Layer Meteorol. 80, 249–282. https://doi.org/10.1007/BF00119545.

Kool, D., Kustas, W.P., Ben-Gal, A., Agam, N., 2021. Energy partitioning between plant canopy and soil, performance of the two-source energy balance model in a vineyard. Agric. For. Meteorol. 300, 108328. https://doi.org/10.1016/j.agrformet.2021.108328.

Kool, D., Agam, N., Lazarovitch, N., Heitman, J.L., Sauer, T.J., Ben-Gal, A., 2014. A review of approaches for evapotranspiration partitioning. Agric. For. Meteorol. 184, 56–70. https://doi.org/10.1016/j.agrformet.2013.09.003.

Kustas, W.P., Alfieri, J.G., Nieto, H., Wilson, T.G., Gao, F., Anderson, M.C., 2018. Utility of the two-source energy balance (TSEB) model in vine and interrow flux partitioning over the growing season. Irrig. Sci. https://doi.org/10.1007/s00271-018-0586-8.

Kustas, W.P., Hatfield, J., Prueger, J.H., 2005. The soil moisture atmosphere coupling experiment (SMACEX): background, hydrometeorological conditions and preliminary findings. J. Hydrometeorol. 6, 791–804. https://doi.org/10.1175/JHM456.1.

Kustas, W.P., Jackson, T.J., Prueger, J.H., Hatfield, J.L., Anderson, M.C., 2003. Remote sensing field experiments for evaluating soil moisture retrieval algorithms and modeling land-atmosphere dynamics in central Iowa. Eos. Trans. Amer. Geophys. Union. 84, 485–493.

Kustas, W.P., Norman, J.M., 1999. Evaluation of soil and vegetation heat flux predictions using a simple two-source model with radiometric temperatures for partial canopy cover. Agric. For. Meteorol. 94 (1), 13–29. https://doi.org/10.1016/S0168-1923(99)00005-2.

Leclerc, M.Y., Foken, T., 2014. Footprints in Micrometeorology and Ecology. Springer-Verlag, Berlin, Heidelberg. https://doi.org/10.1007/978-3-642-54545-0_2.

Mauder, M., Oncley, S.P., Vogt, R., Weidinger, T., Ribeiro, L., Bernhofer, C., Foken, T., Kohsiek, W., De Bruin, H.A.R., Liu, H., 2007. The energy balance experiment EBEX-2000. Part II: intercomparison of eddy-covariance sensors and post-field data processing methods. Bound.-Layer Meteorol. 123, 29–54. https://doi.org/10.1007/s10546-006-9139-4.

Masanganise, J., Kunz, J.R., Clulow, A.D., Mabhaudhi, T., Savage, M.J., 2022. Evapotranspiration estimates of soybean using surface renewal: Comparison with crop coefficient approach. Phys. Chem. Earth 128, 103244. https://doi.org/10.1016/j.pce.2022.103244.

Mölder, M., Grelle, A., Lindroth, A., Halldin, S., 1999. Flux profile relationships over a boreal forest roughness sublayer correction. Agric. For. Meteorol. 98 (99), 645–658. https://doi.org/10.1016/S0168-1923(99)00131-8.

Nieto, H., Kustas, W.P., Torres-Rúa, A., et al., 2019. Evaluation of TSEB turbulent fluxes using different methods for the retrieval of soil and canopy component temperatures from UAV thermal and multispectral imagery. Irrig. Sci. 37, 389–406. https://doi.org/10.1007/s00271-018-0585-9.

Norman, J.M., Kustas, W.P., Humes, K.S., 1995. Source approach for estimating soil and vegetation energy fluxes in observations of directional radiometric surface temperature. Agric. For. Meteorol. 77 (3–4), 263–293. https://doi.org/10.1016/0168-1923(95)02265-Y.

Parry, C.K., Nieto, H., Guillevic, P., Agam, N., Kustas, W.P., Alfieri, J., McKee, L., McElrone, A.J., 2019. An intercomparison of radiation partitioning models in vineyard canopies. Irrig. Sci. https://doi.org/10.1007/s00271-019-00621-x.

Paw U, K.T, Qiu, J., Su, H-B., Watanabe, T., Brunet, Y., 1995. Surface renewal analysis: a new method to obtain scalar fluxes without velocity data. Agric. For. Meteorol. 74, 119–137. https://doi.org/10.1016/0168-1923(94)02182-J.

Priestley, C.H.B., Taylor, R.J., 1972. On the assessment of surface heat flux and evaporation using large-scale parameters. Mon. Weather Rev. 100, 81–92. https://doi.org/10.1175/1520-0493(1972)100>0081:OTAOSH<2.3.CO;2.

Prueger, J.H., Hatfield, J.L., Kustas, W.P., Hipps, L.E., MacPherson, J.I., Neale, C.M.U., Eichinger, W.E., Cooper, D.I., Parkin, T.B., 2005. Tower and aircraft eddy covariance measurements of water vapor, energy, and carbon dioxide fluxes during SMACEX. J. Hydrometerol. 6, 954–960. https://doi.org/10.1175/JHM457.1.

Raupach, M.R., Finnigan, J.J., Brunet, Y., 1996. Coherent eddies in vegetation canopies: The mixing-layer analogy. Bound.-Layer Meteorol. 78, 351–382. https://doi.org/10.1007/BF00120941.

Sánchez, J.M, López-Urrea, R., Valentín, F., Caselles, V., Galve, J.M., 2019. Lysimeter assessment of the simplified two-source energy balance model and eddy covariance system to estimate vineyard evapotranspiration. Agric. For. Meteorol. 274, 172–183. https://doi.org/10.1016/j.agrformet.2019.05.006.

Santos, F., 2018. Assessing olive evapotranspiration partitioning from soil water balance and radiometric soil and canopy temperatures. Agronomy 8, 43. https://doi.org/10.3390/agronomy8040043.

Seo, Y.G., Lee, W.K., 1988. Single-eddy model for random surface renewal. Chem. Eng. Sci. 43 (6), 1395–1402. https://doi.org/10.1016/0009-2509(88)85112-1.

Shuttleworth, W.J., Wallace, J.S., 1985. Evaporation from sparse crops-an energy combination theory. Q. J. R. Meteorol. Soc. 111, 839–855. https://doi.org/10.1256/smsqj.46909.

Song, L., Liu, S., Zhang, X., Zhou, J., Li, M., 2015. Estimating and validating soil evaporation and crop transpiration during the HiWATER-MUSOEXE. IEEE Geosci. Remote Sens. Lett. 12, 334–338. https://doi.org/10.1109/LGRS.2014.2339360.

Spano, D., Snyder, R.L., Duce, P., Paw, U.K.T., 2000. Estimating sensible and latent heat flux densities from grapevine canopies using surface renewal. Agric. For. Meteorol. 104, 171–183. https://doi.org/10.1016/S0168-1923(00)00167-2.

Twine, T.E., Kustas, W.P., Norman, J.M., Cook, D.R., Houser, P.R., Meyer, T.P., Prueger, J.H., Starks, P.J., Wesley, M.L., 2000. Correcting eddy-covariance flux underestimates over grassland. Agric. For. Meteorol. 103, 279–300. https://doi.org/10.1016/S0168-1923(00)00123-4.

Van Atta, C.W., 1977. Effect of coherent structures on structure functions of temperature in the atmospheric boundary layer. Arch. Mech. 91229, 161–171.

Willmott, C.J., Robeson, S.M., Matsuura, K., 1981. Int. J. Climatol. 32 (13). https://doi.org/10.1002/joc.2419.

Zhou, Y., Sühring, M., Li, X., 2023. Evaluation of energy balance closure adjustment and imbalance prediction methods in the convective boundary layer – A large eddy simulation study. Agric. For. Meteorol. 333, 109382. https://doi.org/10.1016/j.agrformet.2023.109382.

Zhu, W., Van Hout, R., Katz, J., 2007. On the flow structure and turbulence during sweep and ejection events in a wind-tunnel model canopy. Bound.-Layer Meteorol. 124, 205–233. https://doi.org/10.1007/s10546-007-9174-9.